Arthritis & Rheumatology
Vol. 76, No. 7, July 2024, pp 1085–1095
DOI 10.1002/art.42830

American College of Rheumatology
Empowering Rheumatology Professionals

A Novel Human Interleukin-23A Overexpressing Mouse Model of Systemic Lupus Erythematosus

Eleni Christodoulou-Vafeiadou,[1] Christina Geka,[1] Lida Iliopoulou,[2] Lydia Ntari,[1] Maria C. Denis,[1] Niki Karagianni,[1] and George Kollias[3]

Objective. Interleukin-23 (IL-23) is a crucial cytokine implicated in chronic inflammation and autoimmunity, associated with various diseases such as psoriasis, psoriatic arthritis, and systemic lupus erythematosus (SLE). This study aimed to create and characterize a transgenic mouse model overexpressing human IL-23A (TghIL-23A), providing a valuable tool for investigating the pathogenic role of human IL-23A and evaluating the efficacy of anti–human IL-23A therapeutics.

Methods. TghIL-23A mice were generated via microinjection of CBA × C57BL/6 zygotes with a fragment of the human *IL23A* gene, flanked by its 5′-regulatory sequences and the 3′ untranslated region of human β-globin. The TghIL-23A pathology was assessed through hematologic and biochemic analyses, cytokine and antinuclear antibody detection, and histopathologic examination of skin and renal tissues. The response to the anti–human IL-23A therapeutic agent guselkumab was evaluated in groups of eight mixed-sex mice receiving subcutaneous treatment twice weekly for 10 weeks using clinical, biomarker, and histopathologic readouts.

Results. TghIL-23A mice exhibited interactions between human IL-23A and mouse IL-23/IL-12p40 and developed a chronic multiorgan autoimmune disease marked by proteinuria, anti–double-stranded DNA antibodies, severe inflammatory lesions in the skin, and milder phenotypes in the kidneys and lungs. The TghIL-23A pathologic features exhibited significant similarities to those observed in human patients with SLE, and they were reversed following guselkumab treatment.

Conclusion. We have generated and characterized a novel genetic mouse model of SLE, providing proof-of-concept for the etiopathogenic role of human IL-23A. This new model has a normal life span and integrates several characteristics of the human disease's complexity and chronicity, making it an attractive preclinical tool for studying IL-23–dependent pathogenic mechanisms and assessing the efficacy of anti–human IL-23A or modeled disease-related therapeutics.

INTRODUCTION

Interleukin-23 (IL-23) is a member of the IL-12 cytokine family, composed of the IL-23A (IL-23p19) and the IL-12/23B (IL-12/23p40) subunits.[1] It is primarily secreted by activated macrophages, dendritic cells, keratinocytes, and other antigen-presenting cells, as well as by T lymphocytes and natural killer cells in peripheral tissues, such as the skin, intestinal mucosa, joints, and lungs.[2–4] Although the IL-23/IL-17 axis has a well-documented protective role against bacterial and fungal infections,[5] its dysregulation can lead to chronic inflammation and autoimmunity, contributing to the development of several diseases, such as psoriasis, psoriatic arthritis, inflammatory bowel disease, rheumatoid arthritis, multiple sclerosis, and others.[5] Because of its significant involvement in various pathogenic conditions, IL-23 has emerged as a promising therapeutic target for

Supported by the use of Biomedical Sciences Research Center (BSRC) Alexander Fleming's Transgenics and Flow Cytometry facilities and by the InfrafrontierGR/Phenotypos Infrastructure (MIS 5002135), funded by the Operational Programme "Competitiveness, Entrepreneurship and Innovation" (NSRF 2014-2020; under the call RESEARCH-CREATE-INNOVATE [T1EΔK-00120; HUPLA]), co-financed by Greece and the European Regional Development Fund of the European Union.

[1]Eleni Christodoulou-Vafeiadou, PhD, Christina Geka, MSc, Lydia Ntari, PhD, Maria C. Denis, PhD, Niki Karagianni, PhD: Biomedcode Hellas SA, Athens, Greece; [2]Lida Iliopoulou, MSc: Biomedical Sciences Research Center (BSRC) Alexander Fleming, Athens, Greece; [3]George Kollias, PhD: BSRC Alexander Fleming, Athens, Greece, and School of Medicine, National and Kapodistrian University of Athens, Athens, Greece.

Additional supplementary information cited in this article can be found online in the Supporting Information section (http://onlinelibrary.wiley.com/doi/10.1002/art.42830).

Author disclosures and graphical abstract are available at https://onlinelibrary.wiley.com/doi/10.1002/art.42830.

Address correspondence via email to George Kollias, PhD, at kollias@fleming.gr.

Submitted for publication July 26, 2023; accepted in revised form February 14, 2024.

chronic inflammatory and autoimmune diseases. Guselkumab, a monoclonal antibody for the treatment of moderate to severe plaque psoriasis, targeting IL-23A, and ustekinumab, a monoclonal antibody for the treatment of Crohn disease, ulcerative colitis, plaque psoriasis, and psoriatic arthritis targeting the common p40 subunit of IL-12 and IL-23, are two of the currently approved biologics that target IL-23, whereas additional biologics targeting IL-23 are also under development.

One autoimmune disease in which IL-23 has recently been shown, both in human patients and mouse models, to play a crucial pathogenic role is systemic lupus erythematosus (SLE). Patients with SLE exhibit elevated IL-23 levels in their serum and plasma, along with increased IL-23 receptor (IL-23R) expression on T cells.[6–10] Conversely, IL-23R deficiency has been found to protect the B6/*lpr* lupus-prone mouse model from lupus development,[11] and treatment of the MRL/*lpr* genetic mouse model of lupus with anti–IL-23A antibodies has been shown to ameliorate lupus symptoms.[12]

SLE is an autoimmune disease characterized by the loss of tolerance against nuclear autoantigens, resulting in complement and cytokine activation and the production of high levels of anti–single-stranded and anti–double-stranded autoantibodies.[13–16] The disease is characterized by the presence of circulating immune complexes that deposit in tissues, leading to multiorgan damage, with kidneys and skin being primarily affected.[15,17–19] Mouse models that replicate key features of SLE pathology have greatly contributed to the study of SLE etiopathogenesis and the identification and validation of potential therapeutic targets.

Among the commonly used mouse models for studying lupus pathology and for the preclinical evaluation of therapeutics, the (NZB × NZW)F1 model exhibits severe lupus-like phenotypes, including splenomegaly, elevated levels of circulating antinuclear antibodies, immune complex–mediated nephritis leading to renal failure, and premature death.[13,20–22] The MRL/*lpr* mouse model, homozygous for the lymphoproliferation spontaneous mutation (Fas^{lpr}), shows defective immune cell apoptosis, leading to the accumulation of double negative autoreactive ($CD4^-CD8^-$) $B220^+$ T cells, the production of anti–double-stranded DNA (anti-dsDNA) autoantibodies, and the development of renal and skin pathologies.[20–22] The BXSB/Yaa mouse model, a recombinant inbred strain, develops lymphoid hyperplasia, nephritis, high serum titers of antinuclear antibodies, and high serum retroviral glycoprotein 70 titers.[20] Additionally, several mouse models based on single-gene knockouts or transgenic expression of specific genes exhibit lupus-like phenotypes, providing insights into the involvement of these genes and functional pathways in SLE mechanisms.[23] Ultimately, although mice spontaneously developing a disease similar to human SLE do not fully recapitulate the complexity of human lupus pathology, they have been an important asset for elucidating the pathogenesis of this disease. Considering the accumulating evidence on the pathogenic role of IL-23, we generated transgenic mice expressing dysregulated human IL-23A (TghIL-23A mice). We demonstrate that TghIL-23A mice develop phenotypes that replicate major clinical, immunologic, and molecular features of human SLE, making them a valid novel mouse model of lupus and a valuable preclinical tool for studying IL-23–dependent pathogenic mechanisms and evaluating therapeutics.

MATERIAL AND METHODS

Generation of TghIL-23A mice. A 2,825 bp genomic DNA fragment containing 986 bp of the human *IL23A* 5′ regulatory sequences and the complete intron-exon sequences up to the stop codon was amplified by polymerase chain reaction (PCR) from the bacterial artificial chromosome CTD-3110H14, and it was further cloned upstream of a 779-bp long DNA fragment containing the 3′ untranslated and polyadenylation sequences of the human β-globin gene.[24] This transgene was microinjected in (CBA × C57BL/6)F2 mouse zygotes and the transgene carriers were identified by PCR using the following primers: F, GTCTTTGCCCATGGAGCAGC, and R, GCCCTTCATAATATCCCCCA. Pronuclear injection of the transgene into fertilized (C57BL/6J × CBA/J)F2 oocytes was performed in the Biomedical Sciences Research Center (BSRC) Alexander Fleming Transgenesis Facility.

Mice and in vivo studies. Wild type, TghIL-23A, TghIL-23A/IL-12B$^{-/-}$,[25] and TghIL-23A/RAG-1$^{-/-}$[26] mice were bred and maintained in a mixed CBA × C57BL/6J genetic background in the animal facilities of Biomedcode Hellas S.A. and BSRC Alexander Fleming under specific pathogen-free conditions. Animals were housed in standard plastic cages with wood chip bedding under an inverted 12:12-hour light/dark cycle at a constant temperature of 22 ± 2°C and relative humidity of approximately 60%. Standard diet and water were provided ad libitum.

For in vivo studies, 10-week-old mice were distributed to sex-balanced groups of 8 to 10 animals and were treated subcutaneously twice weekly for 10 weeks with either saline or different doses of guselkumab (Tremfya; Janssen-Cilag International NV). Mice were monitored regularly to record their weight and skin clinical scores, whereas ear thickness was measured at the completion of the in vivo part of the study. All animal experimentation was approved by the BSRC Alexander Fleming Institutional Committee of Protocol Evaluation in conjunction with the Veterinary Service Management of the Hellenic Republic Prefecture of Attica according to all current European and national legislation and was performed in accordance with relevant guidelines and regulations (approved protocol no. 466365/25.05.22).

Skin clinical score and cytokine and autoantibody detection. The TghIL-23A skin phenotype was assessed based on a scoring scale adapted from the study by Yang et al,[27] with clinical scores representing the sum of three individual scores

assessing (1) the extent of periocular fur loss (0 [normal], 0.5 [mild], and 1 [severe]); (2) the extent of fur thinning and skin redness of the abdominal area (0 [normal], 0.5 [mild], and 1 [severe]); and (3) the severity of the ventral neck and thorax area pathology (0 [normal], 0.5 [mild lesions in the neck area], 1 [mild to moderate lesions extending toward the thorax], and 2 [severe extended skin lesions with serous exudates and crusts]). Ear thickness was measured using an electronic caliper. Cytokines were measured in skin tissue lysates using the LEGENDplex Mouse Inflammation Panel (13-plex) according to the manufacturer's instructions. Serum levels of anti-dsDNA, anti–single-stranded DNA (anti-ssDNA), anti-SSA/Ro52 antibodies, and total IgG were assessed by enzyme-linked immunosorbent assay (ELISA) (Alpha Diagnostic International, 5120; Alpha Diagnostic International, 5320; Alpha Diagnostic International, 5730; and Abcam, ab157719, respectively) according to the manufacturer's instructions. Serum from an MRL/*lpr* mouse with severe proteinuria (Hooke Laboratories, cat No. LZ-0201) was used as positive control for anti-dsDNA and anti-SSA/Ro52 ELISA.

Hematologic and urine analysis and flow cytometry of skin samples. Red blood cell (RBC) counts, hematocrit (HCT) levels, and hemoglobin levels were measured using the BC-5000 Vet Hematology Analyzer (Mindray Animal Medical). Urine protein concentrations were assessed using either the AU480 Clinical Chemistry Analyzer (Beckman Coulter) or the Multistix 10 SG (Series 2300; Siemens). Skin samples collected from the ventral neck area of four to five mice were minced in Hank's balanced solution (HBSS) and incubated at 4°C overnight with 1.5 mg/mL of dispase II (Roche; 04942078001). The next day, samples were incubated at 37°C with 1 mg/mL of collagenase IV (C5138; Sigma-Aldrich) and 10% fetal bovine serum (FBS) for 1.5 hours while shaking. Following this incubation, the samples were vortexed, filtered through a 70-μm cell strainer, washed with HBSS plus 10% FBS, and centrifuged at 1,200 revolutions per minute. The cell pellet was resuspended in a fluorescence-activated cell sorting (FACS) buffer, and 1.5×10^6 cells per sample were stained with the viability dye Zombie-NIR (Biolegend) and with specific antibodies for the detection of CD4, CD8, B220, CD11b, Ly-6G, F4/80, and SinglecF (BioLegend); finally, the samples were analyzed by flow cytometry using BD FACSCanto II and BD FACSDiva software (BD Biosciences).

Histopathology and immunohistochemistry. Tissue paraffin sections were stained with hematoxylin and eosin (H&E) for histopathologic evaluation or with biotinylated anti–mouse-IgG (BA-9200; Vector Laboratories) for the detection of immune complex deposits and anti–human IL-23A (AM20386PU-N; OriGene) for the detection of human IL-23A protein in various tissues. Skin and ear histopathologic evaluation was performed in a masked manner using a scoring scale adapted from the study by Yang et al.[27] Scores are the sum of the individual scores of epidermis and dermis pathology. Epidermis pathology is characterized by hyperkeratosis or orthokeratosis and acanthosis leading to tissue destruction and necrosis assessed in a scale from 0 to 4, and dermis pathology includes immune cell infiltration in the different dermis layers assessed in a scale ranging from 0 to 3. Lung histopathologic evaluation was also performed in a masked manner using a scoring scale adapted from the study by Bell et al.[28] Scores are the sum of the individual scores of peribronchial and perivascular inflammation (scale 0–3) along with interstitial inflammation (scale 0–3).

RNA isolation, PCR analysis, and statistical analysis. Tissue RNA was isolated with Trizol (15596026; ThermoFisher Scientific) and reverse transcribed with Moloney murine leukemia virus reverse transcriptase (M1705; Promega). The expression of human IL-23A messenger RNA and β_2-microglobulin (β_2m) was assessed by PCR using specific primers (hIL-23AF: GTCTTTGCCCATGGAGCAGC; hIL-23AR: GCCCTTCATAATA TCCCCCA; mβ_2mF: TTCTGGTGCTTGTCTCACTGA; and mβ_2mR: CAGTATGTTCGGCTTCCCATTC). Data are presented as mean ± SEM, and Student's *t*-test was used for the evaluation of statistical significance, with P values < 0.05 being considered statistically significant. More specifically, normality and lognormality tests were performed using the Kolmogorov-Smirnov test, the Shapiro-Wilk test, and the D'Agostino and Pearson normal Gaussian distribution. If sample values passed all three tests, the unpaired parametric Student's *t*-test was chosen. If not, the nonparametric Mann-Whitney *U* test was used. Analysis was performed using Prism V.10 (GraphPad).

RESULTS

Generation of TghIL-23A mice. To examine the pathogenic role of IL-23A, we generated TghIL-23A mice. The transgene used contained a fragment of the human *IL-23A* gene locus composed of 5′ regulatory sequences sufficient to confer regulated transcription[29] of the complete intron-exon sequences that followed. The fragment was cloned upstream of a nonregulated 3′ untranslated region to enable the abolishment of the post-transcriptional regulation of IL-23A and its altered expression, aiming to increase the risk of development of a pathogenic condition[30] (Figure 1A). The TghIL-23A mice generated were maintained in CBA × C57BL/6 background, and the expression of the human *IL-23A* transgene was confirmed by PCR in the skin, lymph nodes, spleen, lungs, and kidneys (Figure 1 B). The human IL-23A protein was also detected by immunohistochemistry in the skin, showing a diffuse positive staining in the dermis, in the cortex of the lymph nodes, in the red pulp of the spleen, in the peribronchial and perivascular areas as well as the interstitium of the lungs and in the glomeruli of the kidneys (Figure 1C).

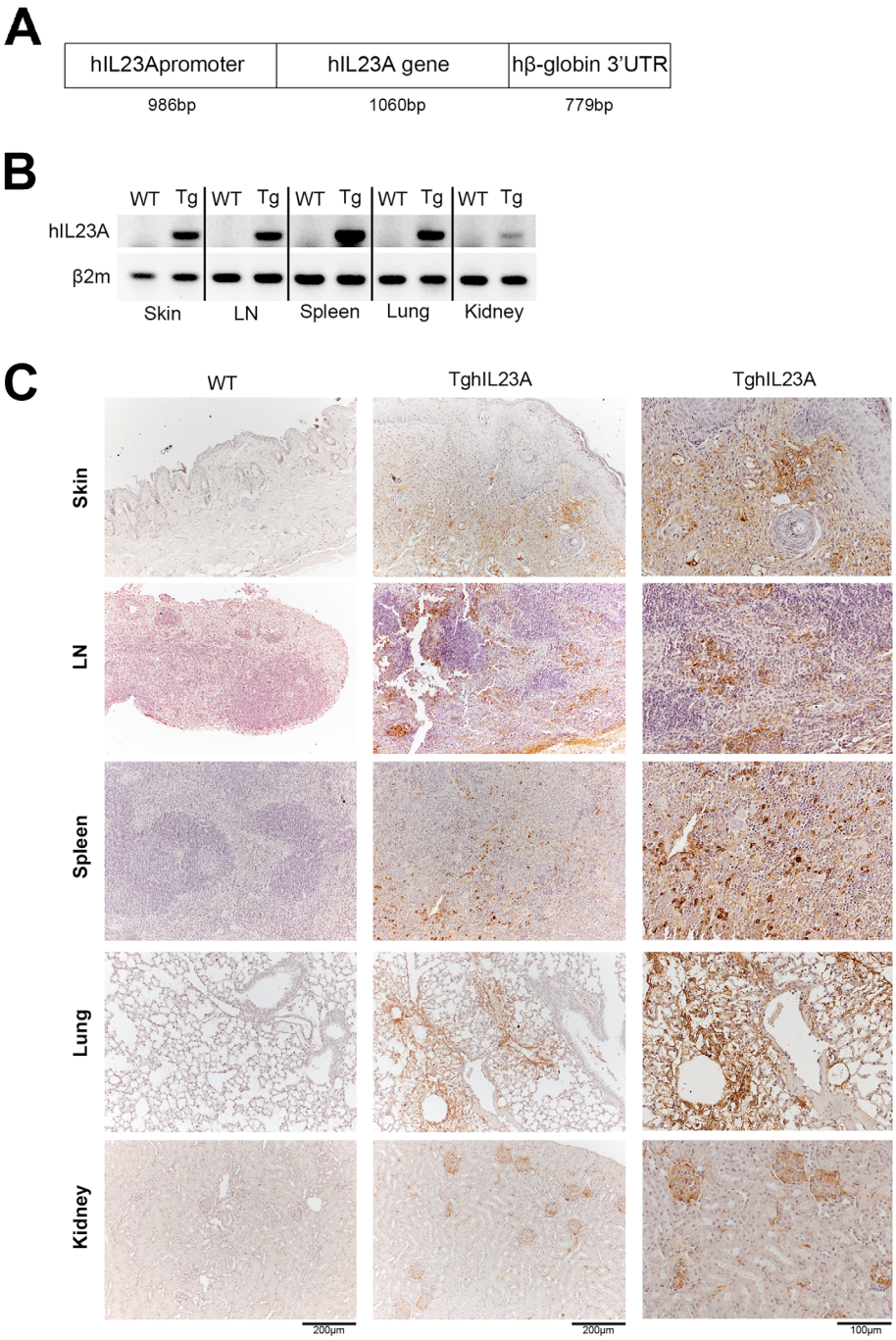

Figure 1. Generation of TghIL-23A mice and hIL-23A expression. (A) Schematic representation of the hIL-23A transgene. (B) hIL-23A mRNA detected by PCR and (C) hIL-23A protein detected by immunohistochemistry in the skin, cervical lymph nodes, spleen, lung, and kidney of TghIL-23A mice. Scale bars = 200 μm and 100 μm. β2m, β_2-microglobulin; hβ-globin, human beta-globin; hIL-23A, human interleukin-23A; LN, lymph node; mRNA, messenger RNA; PCR, polymerase chain reaction; Tg, transgenic; TghIL-23A, transgenic human interleukin-23A; UTR, untranslated region; WT, wild type. Color figure can be viewed in the online issue, which is available at http://onlinelibrary.wiley.com/doi/10.1002/art.42830/abstract.

Human IL-23A expression leads to a spontaneous and progressive skin pathology with immune system involvement. TghIL-23A mice are fertile, have a normal life span, and exhibit normal body weight gain until the age of 7 months, when they start to show a progressive body weight loss (Supplementary Fig 1), with no significant difference in overall survival up to an observation period of 40 weeks. At four weeks of age, the TghIL-23A mice start developing clinical symptoms of skin pathology, which first manifest as fur thinning in the periocular and abdominal areas (Figure 2A, panels i and iv). As the disease progresses, the clinical symptoms become more severe and include the thickening of the ear pinna (Figure 2A, panels v and

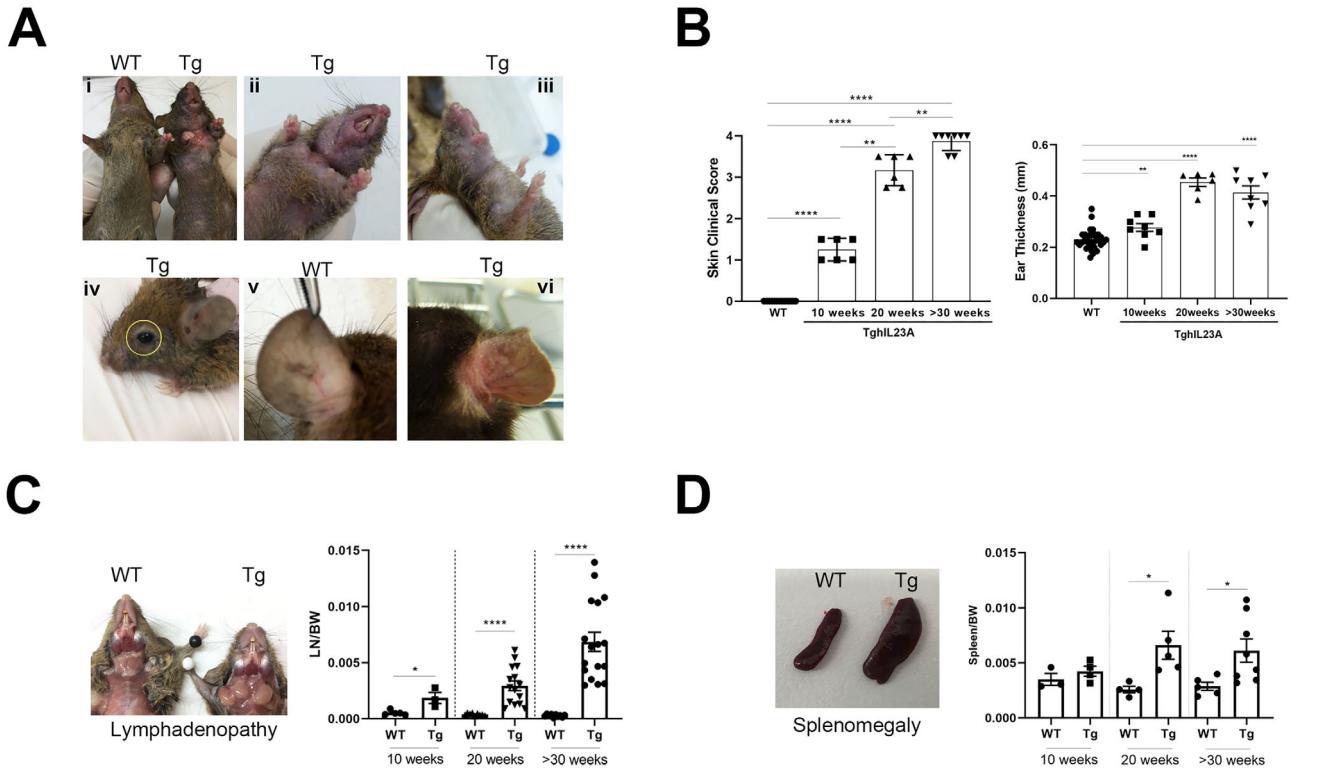

Figure 2. Clinical features of dermatitis, splenomegaly, and lymphadenopathy in the TghIL-23A mice. (A) Macroscopic images of 30-week-old TghIL-23A and WT littermate mice depicting clinical features of fur thinning and skin lesions in the ventral–thoracic (i–iii) and periocular areas (iv) as well as in the ears of the Tg mice (v–vi). (B) Clinical assessment and ear thickness measurements show an age-dependent increased severity of the TghIL-23A skin pathology (n = 6–8 mice per group). The assessment of the LN and spleen to BW ratios show the development of a TghIL-23A age-dependent (C) lymphadenopathy (n = 3–17 mice per group) and (D) splenomegaly (n = 3–9 mice per group). Data are presented as mean ± SEM; $^{*}P < 0.05$; $^{**}P < 0.005$; $^{***}P < 0.0002$; $^{****}P < 0.0001$. BW, body weight; hIL-23A, human interleukin-23A; LN, lymph node; Tg, transgenic; TghIL-23A, transgenic human interleukin-23A; WT, wild type. Color figure can be viewed in the online issue, which is available at http://onlinelibrary.wiley.com/doi/10.1002/art.42830/abstract.

vi) as well as the extensive loss of fur and the appearance of skin lesions with serous exudate production and crust formation in the rostrum and the ventral neck and/or upper thorax (Figure 2A, panels ii and iii).

The progression of the clinical phenotype was assessed using a scoring scale of four points, taking into account the features of the pathology developing in the periocular, abdominal, ventral neck, and thorax areas. By the age of 10 weeks, all the animals developed mild skin pathology that reached a maximum score by 30 weeks of age (Figure 2B). The clinical signs also included the involvement of the immune compartment, as indicated by the hyperplastic phenotype observed in the draining lymph nodes of the affected ventral neck area (Figure 2C) as well as the greatly enlarged spleens of 5- to 7-month-old mice (Figure 2D).

Mice expressing human IL-23A develop autoimmune lupus pathology. To further assess the clinical profile of the TghIL-23A mice, we performed hematologic and biochemic analysis of the blood and urine of 20- to >35-week-old mice. Analysis of the blood of 20-week-old TghIL-23A mice showed significantly reduced RBC counts as well as reduced HCT and hemoglobin levels, indicating an anemic phenotype (Figure 3A). Moreover, urine analysis showed that the TghIL-23A mice exhibited proteinuria indicated by the increased albumin to creatinine ratio, suggesting mild renal dysfunction (Figure 3B).

The finding of anemia, which is a common sign of chronic inflammatory conditions, such as autoimmune pathologies and proteinuria, that implicates impaired renal function, suggested that the TghIL-23A phenotype could possibly be linked with autoimmunity. To explore this possibility, we assessed key features of autoimmunity, including the presence of circulating autoantibodies as well as the T cell and B cell involvement. We therefore screened serum samples of wild-type and TghIL-23A mice at different ages for the detection of antinuclear antibodies and total immunoglobulin levels. The serum samples of TghIL-23A mice from 10 weeks of age tested positive for both anti-ssDNA (Supplementary Fig 2A) and anti-dsDNA antibodies (Figure 3C). Furthermore, low levels of anti-SSA/Ro52 in serum samples of TghIL-23A mice were detected at the age of 20 weeks and were further increased at the age of 36 weeks, albeit without reaching statistical significance (Supplementary Fig 2B). IgG levels were significantly increased in circulation (Figure 3D), and IgG was deposited in the renal glomeruli, where increased numbers of

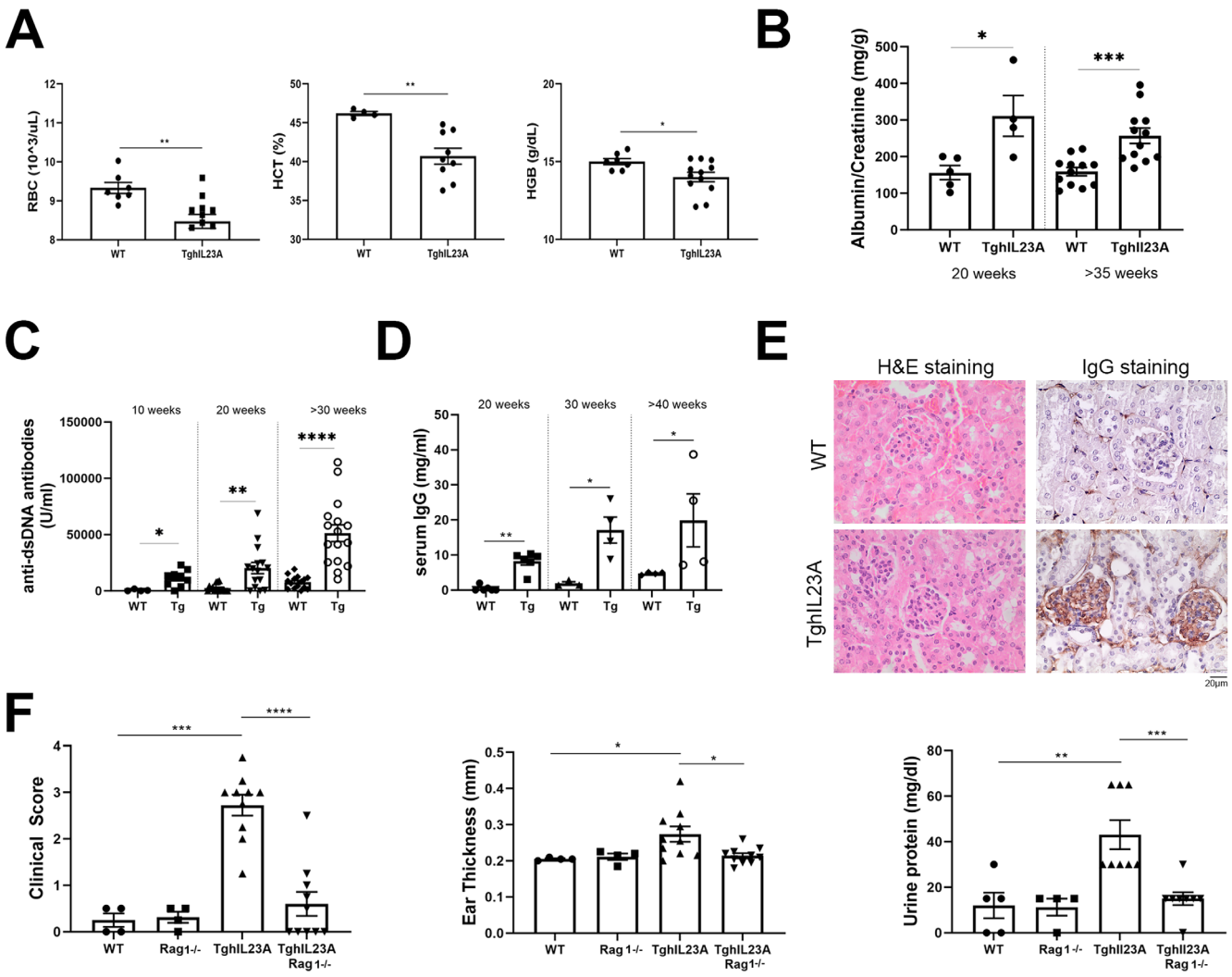

Figure 3. TghIL-23A mice develop an autoimmune lupus-like pathology. Twenty-week-old TghIL-23A mice show (A) signs of anemia evident by the reduced RBC counts, HCT levels, and HGB levels (n = 4–12 mice per group); (B) mild proteinuria evident by the increased ratio of albumin/creatinine urine levels (n = 4–12 mice per group); (C) increased circulating levels of anti-dsDNA antibodies (n = 4–16 mice per group); and (D) total IgG (n = 3–6 mice per group) and (E) mild mesangial hypercellularity and IgG deposits in their glomeruli. Scale bar = 20 μm. (F) The TghIL-23A clinical pathology features of 20-week-old mice are abolished following their crossing to RAG-1$^{-/-}$ mice (n = 4–10 mice per group). Data are presented as mean ± SEM; *P < 0.05; **P < 0.005; ***P < 0.0002; ****P < 0.0001. anti-dsDNA, anti–double-stranded DNA; HCT, hematocrit; H&E, hematoxylin and eosin; HGB, hemoglobin; RBC, red blood cell; Tg, transgenic; TghIL-23A, transgenic human interleukin-23A; WT, wild type. Color figure can be viewed in the online issue, which is available at http://onlinelibrary.wiley.com/doi/10.1002/art.42830/abstract.

mesangial cells were also detected (Figure 3E). Crossing the TghIL-23A mice to RAG-1$^{-/-}$ mice resulted in complete abolishment of the skin pathology and the proteinuria (Figure 3F), confirming the critical involvement of B and T lymphocytes.

Crossing the TghIL-23A mice with the IL-12B–deficient mice (TghIL-23A/IL-12B$^{-/-}$) resulted in significant decreases of circulating anti-dsDNA antibodies (Supplementary Fig 3A) and decreased proteinuria (Supplementary Fig 3B) in 20-week-old mice. These data suggest that the pathology is driven by an IL-23 dimer, composed of a human IL-23A and a mouse IL-12B subunit. The simultaneous manifestation of inflammation in the skin, the impaired renal function, and anemia together with the presence of antinuclear antibodies and the dependency of the pathology on T cells and B cells as well as on the expression of the IL-12B subunit support that TghIL-23A mice reproduce key features of systemic lupus autoimmunity[15,31–33] that are IL-23 dependent.

TghIL-23A mice develop cutaneous lupus with pulmonary manifestations. We next studied in greater detail the skin pathology and its connection with the autoimmune lupus developing in these mice. Histopathologic analysis of H&E-stained sections of the affected skin of 20- to 30-week-old TghIL-23A mice revealed the presence of vacuolar interface dermatitis (Figure 4A, panel i), acanthosis of the epidermis with elongated rete ridges and orthokeratosis (Figure 4A, panel ii),

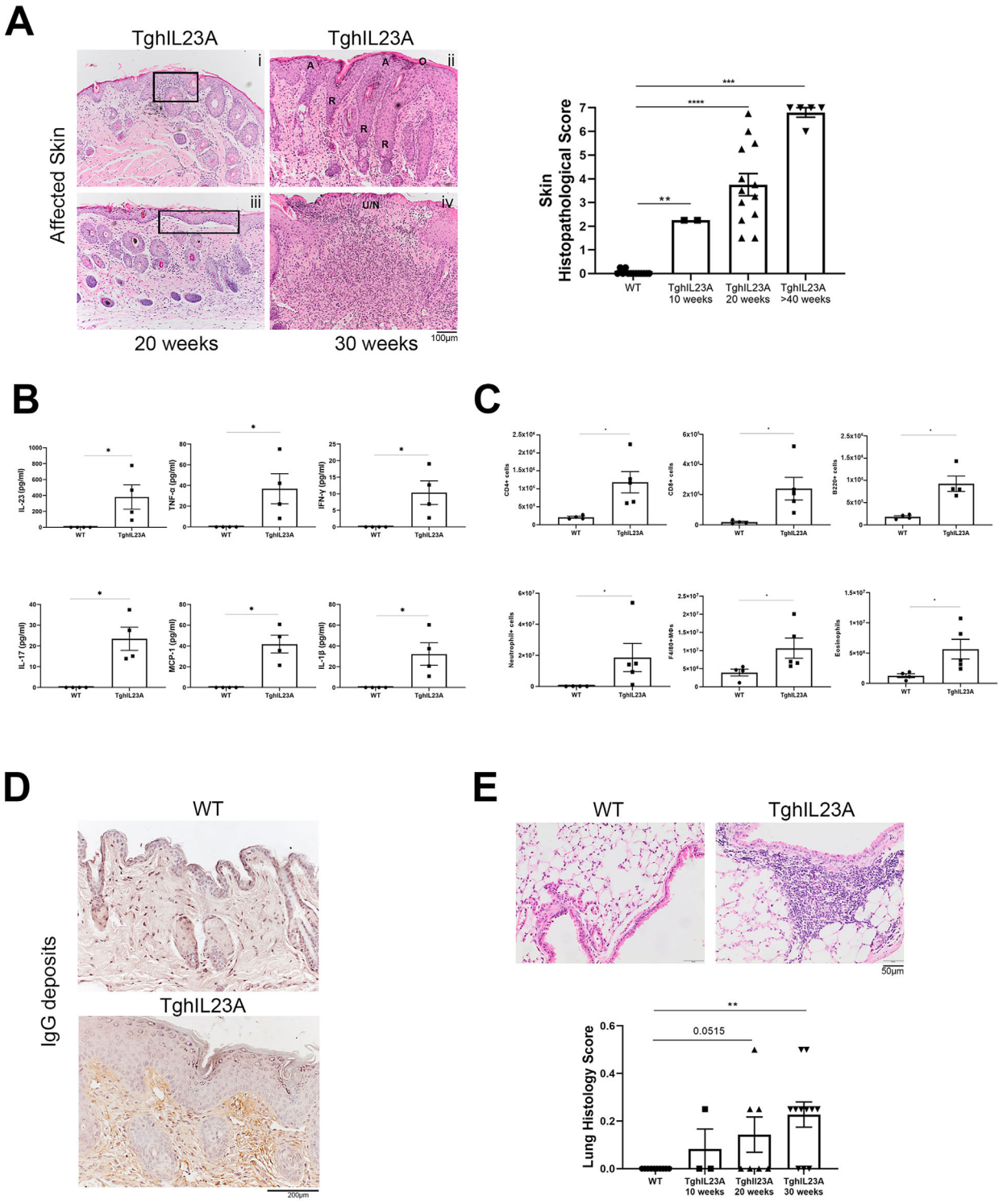

Figure 4. Histopathologic analysis of the cutaneous and lung manifestations of the TghIL-23A pathology (A) H&E-stained paraffin sections showing (i) vacuolar interface dermatitis; (ii) orthokeratosis (O), acanthosis (A), and rete ridges formation (R); (iii) and epidermolysis as well as accumulation of inflammatory cells (PMNs); and (iv) ulcerations and necrosis (U/N) in the skin of TghIL-23A mice. Scale bar = 100 μm. These pathologic features become progressively more severe in older mice (graph) (n = 2–13 mice per group). (B) The affected skin of 20-week-old TghIL-23A mice also exhibit increased levels of inflammatory cytokines (n = 4 mice per group), (C) lymphoid and myeloid infiltrates (n = 4–5 mice per group), and (D) IgG deposits. Scale bar = 200 μm. (E) representative H&E-stained lung paraffin sections showing evidence of interstitial and peribronchial lung inflammation in 20-week-old TghIL-23A mice that are also assessed for their severity histopathologically (graph) (n = 4–5 mice per group). Scale bar = 50 μm. Data are presented as mean ± SEM; $^{*}P < 0.03$; $^{**}P < 0.0095$; $^{***}P = 0.0001$; $^{****}P < 0.0001$. H&E, hematoxylin and eosin; IFNγ, interferon-γ; IL, interleukin; MCP-1, monocyte chemotactic protein 1; TghIL-23A, transgenic human interleukin-23A; TNFα, tumor necrosis factor α; WT, wild type. Color figure can be viewed in the online issue, which is available at http://onlinelibrary.wiley.com/doi/10.1002/art.42830/abstract.

epidermolysis (Figure 4A, panel iii), accumulation of inflammatory cells (polymorphonuclear cells [PMNs]), and ulcerations and necrosis in the dermis (Figure 4A, panel iv). Similar (but slightly milder in severity) pathologic features were observed in the ears of these mice that showed hyperkeratosis, acanthosis, and accumulation of inflammatory cells (PMNs) in the subepidermal layer (Supplementary Fig 4A).

The severity and progression of the skin pathology was monitored using a scoring scale of seven points assessing histopathologic features present in the epidermis and dermis layers of the affected skin. In all the TghIL-23A animals examined, mild skin and ear histologic features were detected by the age of 10 weeks, whereas scores reached maximum severity by the age of 40 weeks (Figure 4A and Supplementary Fig 4B). Interestingly, similar to what we observed with the clinical features, the histopathologic features in the skin were also abolished when the TghIL-23A mice were crossed with RAG-1$^{-/-}$ mice and with IL-12B$^{-/-}$ mice (Supplementary Fig 5A and B), highlighting again the dependency on the IL-23 pathogenic pathway and the adaptive immune response.

Cytokine and chemokine multiplex analysis revealed that the local skin inflammatory milieu contained increased levels of multiple inflammatory molecules, such as IL-23, tumor necrosis factor α (TNFα), interferon-γ (IFNγ), IL-17A, monocyte chemotactic protein 1 (MCP-1), and IL-1b (Figure 4B). FACS analysis indicated the accumulation of inflammatory cells in the affected skin, which included primarily CD4^{+} and CD8^{+} T cells, B220^{+} B cells, and F4/80^{+} macrophages, neutrophils, and eosinophils (Figure 4C). In accordance with the accumulation of B cells in the skin of TghIL-23A mice, extensive IgG deposits were detected in the upper dermis area (Figure 4D) but not in the dermal or epidermal interface, as often observed in human patients.

Because lupus can affect multiple organs, we performed histopathologic analysis of H&E-stained sections of the ileum, colon, heart, and lungs, organs that are known to be affected by lupus, and of these, only the lungs showed interstitial and peribronchial inflammation (Figure 4E and Supplementary Fig 6). The percentage of TghIL-23A mice with pathologic findings in their lungs increased in older mice. At 10 weeks of age, only 33% of the mice showed lung inflammation, whereas 57% of mice at 20 weeks of age and 73% of mice at 30 weeks of age were affected in their lungs (Figure 4E). Interestingly, the skin histopathologic findings and the local inflammatory milieu together with the pathologic manifestations in the lungs bear similarities to most of the pathologic features observed in human patients with cutaneous lupus.[19,32,34–37]

Human IL-23A blockade acts therapeutically and ameliorates TghIL-23A cutaneous lupus. The response and dependency of the TghIL-23A lupus pathology on the expression of the human IL-23A subunit was further studied by treating the mice with guselkumab, a monoclonal antibody that specifically targets and blocks this subunit. Age- and sex-matched groups of TghIL-23A mice with similar body weights, skin pathology, and proteinuria were treated for 10 weeks, starting from 10 weeks of age, with either 5 or 15 mg/kg of guselkumab, which was administered subcutaneously twice weekly. Clinical monitoring indicated that both doses of guselkumab could significantly reduce the severity of the skin pathology, whereas only the highest dose could significantly reduce the ear thickness (Figure 5A). Nevertheless, skin and ear histopathologic scores were significantly reduced by both doses (Figure 5B).

Similarly, treatment with the highest dose of guselkumab restored the size of the draining lymph nodes and the spleens of the TghIL-23A mice to normal levels (Figure 5C) and returned the urine protein to wild-type levels (Figure 5D), whereas both the 5 and 15 mg/kg doses of guselkumab also efficiently reduced the levels of circulating IgG (Figure 5E). Finally, treatment with guselkumab efficiently reduced the percentage of IgG-positive glomeruli in the kidneys of TghIL-23A mice. More specifically, although untreated transgenic mice presented with 76% IgG-positive glomeruli, following treatment with 5 of mg/kg guselkumab only 34% of the glomeruli stained positive for IgG and following treatment with 15 of mg/kg guselkumab this percentage dropped to 20% (Figure 5F).

DISCUSSION

The TghIL-23A mice were generated with the aim of developing a novel mouse model to study the role of deregulated human IL-23A expression in pathogenesis. The implication of IL-23A deregulation in pathogenic mechanisms has been previously supported by the phenotypes developed in mice lacking the RNA-binding protein tristetrapolin (TTP), a posttranscriptional regulator of both TNFα and IL-23A. TTP knockout mice spontaneously develop systemic autoimmunity, with features of arthritis, cardiac valvulitis, dermatitis, and renal pathology, accompanied by high titers of anti-dsDNA and anti-ssDNA autoantibodies.[38–40] 40 Because transgenic mice expressing deregulated human TNF were shown to develop arthritis and cardiac valvulitis,[41] we questioned whether the deregulated expression of human IL-23A could similarly lead to the development of the remaining phenotypes occurring in the TTP$^{-/-}$ mice.

TghIL-23A mice were shown to exhibit an overt skin phenotype that included signs of alopecia, as well as the development of erythema and eczematous lesions with histopathologic findings of acanthosis and inflammatory cell infiltration, which are typical signs of dermatitis. Cytokine analysis revealed the local upregulation of IL-17A that is consistent with the expected activation of the IL-23/IL-17 axis in these mice.[42,43] Additionally, increased levels of TNF, IL-1β, and IFNγ cytokines commonly associated with skin inflammation were observed.[42,44] Although the skin pathology developing in TghIL-23A mice shares several similarities with IL-23/IL-17–driven psoriasis,[42] it also exhibits nontypical features

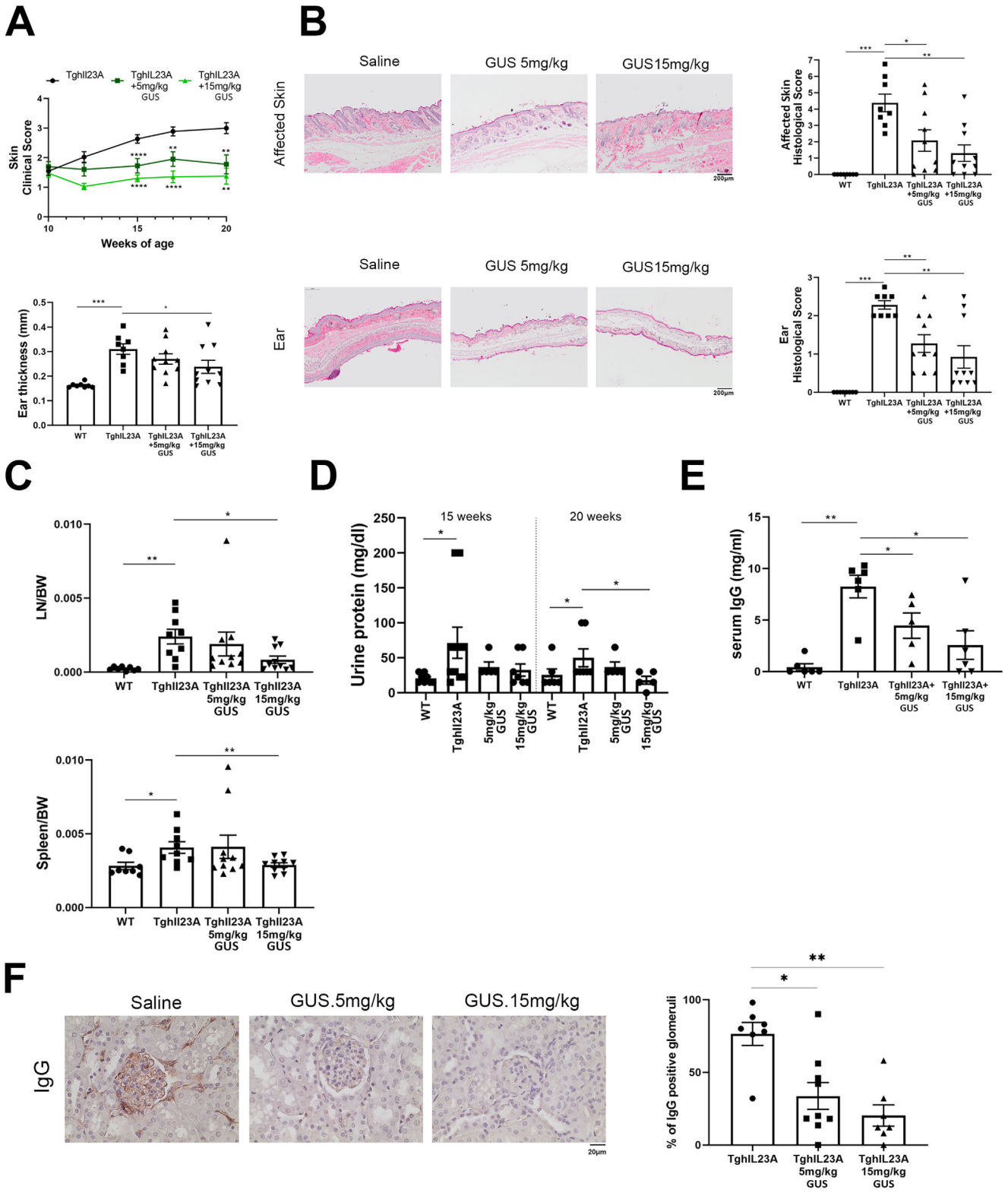

Figure 5. Dose-dependent amelioration of the TghIL-23A lupus pathology following IL-23A blockade. Reduced skin (upper panel) and ear (lower panel) (A) clinical and (B) histopathologic signs (n = 8–11 mice per group), (C) reduced LN/BW and spleen/BW ratios (n = 8–10 mice per group), (D) urine protein levels (n = 5–10 mice per group), (E) IgG circulating levels (n = 5–6 mice per group), and (F) glomerular IgG deposits (n = 7–9 mice per group) following a 10-week-long treatment of TghIL-23A mice with anti-human IL-23A (GUS). Scale bar = 20 µm. Data are presented as mean ± SEM; *$P < 0.04$; **$P < 0.0092$; ***$P = 0.0002$; ****$P < 0.0001$. BW, body weight; GUS, guselkumab; IL-23A, interleukin-23A; LN, lymph node; TghIL-23A, transgenic human interleukin-23A; WT, wild type.

of psoriasis, such as vacuolar interface dermatitis, orthokeratosis, epidermal thinning, epidermolysis, and the localized accumulation of IgG deposits, features that resemble those observed in human patients and mouse models of autoimmune skin disorders.[27,37] Furthermore, the presence of $B220^+$ cells infiltrating the inflamed skin, as well as the enlarged local lymph nodes and spleens, suggests the involvement of an autoimmune component in the TghIL-23A driven pathology.

Several lines of evidence support the pathogenic involvement of IL-23A in SLE. Specifically, high serum levels of IL-23 have been detected in patients with SLE, and IL-23R–deficient lupus-prone mice (B6/*lpr*) are protected from lymphoproliferation, anti-dsDNA antibody production, and nephritis.[11,45] Additionally, treatment of lupus-prone mice with anti-IL-23 antibodies has been shown to ameliorate lupus nephritis.[12]

In agreement with the previously mentioned evidence, our work revealed great similarities between the clinical and histopathologic findings of TghIL-23A mice and those observed in human patients with SLE.[16,37] More specifically, the presence of skin pathology, of inflammatory kidney infiltrates, and of interstitial and/or peribronchial lung inflammation, as well as the increased circulating levels of antinuclear autoantibodies and the local deposition of immunoglobulins in tissues, are key SLE pathology features. Importantly, these pathologic findings were shown to be T and B cell dependent because they were all ameliorated in a RAG-$1^{-/-}$ context, further confirming the involvement of an autoimmune component in the pathology of TghIL-23A mice. IL-23A may partner either with the IL-23/IL-12B subunit to form the IL-23 cytokine or with the Epstein-Barr virus–induced gene 3 subunit to form the IL-39 cytokine, both of which have been linked to SLE pathogenesis.[1,46] Our work revealed that the SLE-related pathology of TghIL-23A mice was abolished when crossed with IL-23/IL-12B–deficient mice, therefore confirming that human IL-23A exerts its pathologic effect through dimerization with IL-23/IL-12B and the formation of the IL-23 cytokine.

The TghIL-23A pathology closely resembles that of the MRL/*lpr* mouse, one of the most commonly used models of SLE, with shared similarities including the features of cutaneous involvement, splenomegaly, lymphadenopathy, autoantibody formation, and renal pathology. Nonetheless, the TghIL-23A model is differentiated from the MRL/*lpr* model in that it exhibits lower levels of autoantibodies (anti-SSA/Ro52 and anti-dsDNA) (Supplementary Fig 7), slower-developing mild renal pathology, and lack of early lethality, thus offering an extended time frame for the study of the disease and its response to treatment. Additionally, the TghIL-23A model allows the direct evaluation of human biologics targeting human IL-23A because we have shown that treatment with the anti–human IL-23A–targeting biologic guselkumab ameliorates the disease. Furthermore, this could be a useful model for testing therapeutic approaches targeting additional components of the IL-23 pathogenic pathway. Overall, with the generation of the TghIL-23A mice, we show that the human IL-23A subunit dimerizes with the mouse IL-23/IL-12B subunit, leading to the development of a lupus-like multiorgan autoimmune disease, characterized by autoantibody production and the formation of inflammatory lesions primarily in the skin, kidneys, and lungs. This novel mouse model provides the proof-of-concept for the etiopathogenic role of IL-23A in lupus and can serve as a valuable tool for studying the mechanisms underlying autoimmunity and for testing novel therapeutic approaches.

ACKNOWLEDGMENTS

The authors thank Marianna Ragkousi for her help in processing and staining histologic samples and Philippos Charalampous for his help in TghIL-23A Rag1$^{-/-}$ mice breeding and maintenance.

AUTHOR CONTRIBUTIONS

All authors were involved in drafting the article or revising it critically for important intellectual content, and all authors approved the final version to be published. Dr Kollias had full access to all of the data in the study and takes responsibility for the integrity of the data and the accuracy of the data analysis.

Study conception and design. Christodoulou-Vafeiadou, Denis, Karagianni, Kollias.

Acquisition of data. Christodoulou-Vafeiadou, Geka, Iliopoulou, Ntari.

Analysis and interpretation of data. Christodoulou-Vafeiadou, Geka, Iliopoulou, Ntari, Denis, Karagianni, Kollias.

REFERENCES

1. Oppmann B, Lesley R, Blom B, et al. Novel p19 protein engages IL-12p40 to form a cytokine, IL-23, with biological activities similar as well as distinct from IL-12. Immunity 2000;13:715–725.
2. Brentano F, Ospelt C, Stanczyk J, et al. Abundant expression of the interleukin (IL)23 subunit p19, but low levels of bioactive IL23 in the rheumatoid synovium: differential expression and toll-like receptor-(TLR) dependent regulation of the IL23 subunits, p19 and p40, in rheumatoid arthritis. Ann Rheum Dis 2009;68:143–150.
3. Goldberg M, Nadiv O, Luknar-Gabor N, et al. Synergism between tumor necrosis factor alpha and interleukin-17 to induce IL-23 p19 expression in fibroblast-like synoviocytes. Mol Immunol 2009;46: 1854–1859.
4. McKenzie BS, Kastelein RA, Cua DJ. Understanding the IL-23–IL-17 immune pathway. Trends Immunol 2006;27:17–23.
5. Schinocca C, Rizzo C, Fasano S, et al. Role of the IL-23/IL-17 pathway in rheumatic diseases: an overview. Front Immunol 2021;12: 637829.
6. Dai H, He F, Tsokos GC, et al. IL-23 Limits the production of IL-2 and promotes autoimmunity in lupus. J Immunol 2017;199:903–910.
7. Puwipirom H, Hirankarn N, Sodsai P, et al. Increased interleukin-23 receptor+T cells in peripheral blood mononuclear cells of patients with systemic lupus erythematosus. Arthritis Res Ther 2010;12:R215.
8. Wong CK, Lit LCW, Tam LS, et al. Hyperproduction of IL-23 and IL-17 in patients with systemic lupus erythematosus: implications for Th17-mediated inflammation in auto-immunity. Clin Immunol 2008; 127:385–393.
9. Xiong DK, Shi X, Han MM, et al. The regulatory mechanism and potential application of IL-23 in autoimmune diseases. Front Pharmacol 2022;13:13:982238.

10. Larosa M, Zen M, Gatto M, et al. IL-12 and IL-23/Th17 axis in systemic lupus erythematosus. Exp Biol Med (Maywood) 2019;244:42–51.
11. Kyttaris VC, Zhang Z, Kuchroo VK, et al. Cutting edge: IL-23 receptor deficiency prevents the development of lupus nephritis in C57BL/6– lpr/lpr mice. J Immunol 2010;184:4605–4609.
12. Kyttaris VC, Kampagianni O, Tsokos GC. Treatment with anti-interleukin 23 antibody ameliorates disease in lupus-prone mice. Biomed Res Int 2013;2013:861028.
13. Theophilopouos AN, Dixon FJ. Murine models of systemic lupus erythematosus. Adv Immunol 1985;37:269–390.
14. Deng GM, Liu L, Kyttaris VC, et al. Lupus serum IgG induces skin inflammation through the TNFR1 signaling pathway. J Immunol 2010;184:7154–7161.
15. Rahman A, Isenberg DA. Systemic lupus erythematosus. N Engl J Med 2008;358:929–939.
16. Kiriakidou M, Ching CL. Systemic lupus erythematosus. Ann Intern Med 2020;172:ITC81–ITC96.
17. Jost SA, Tseng LC, Matthews LA, et al. IgG, IgM, and IgA antinuclear antibodies in discoid and systemic lupus erythematosus patients. ScientificWorldJournal 2014;2014:171028.
18. Kolkhir P, Pogorelov D, Olisova O, et al. Comorbidity and pathogenic links of chronic spontaneous urticaria and systemic lupus erythematosus—a systematic review. Clin Exp Allergy 2016;46:275–287.
19. Tsokos GC. Autoimmunity and organ damage in systemic lupus erythematosus. Nat Immunol 2020;21:605–614.
20. Li W, Titov AA, Morel L. An update on lupus animal models. Curr Opin Rheumatol 2017;29:434–441.
21. Pathak S, Mohan C. Cellular and molecular pathogenesis of systemic lupus erythematosus: lessons from animal models. Arthritis Res Ther 2011;13:241.
22. Andrews BS, Eisenberg RA, Theofilopoulos AN, et al. Spontaneous murine lupus-like syndromes. Clinical and immunopathological manifestations in several strains. J Exp Med 1978;148:1198–1215.
23. Morel L. Genetics of SLE: evidence from mouse models. Nat Rev Rheumatol 2010;6:348–357.
24. Kollias G, Hurst J, deBoer E, et al. The human β-globin gene contains a downstream developmental specific enhancer. Nucleic Acids Res 1987;15:5739–5747.
25. Magram J, Connaughton SE, Warrier RR, et al. IL-12-deficient mice are defective in IFN gamma production and type 1 cytokine responses. Immunity 1996;4:471–481.
26. Mombaerts P, Iacomini J, Johnson RS, et al. RAG-1-deficient mice have no mature B and T lymphocytes. Cell 1992;68:869–877.
27. Yang JQ, Chun T, Liu H, et al. CD1d deficiency exacerbates inflammatory dermatitis in MRL-lpr/lpr mice. Eur J Immunol 2004;34:1723–1732.
28. Bell RD, Wu EK, Rudmann CA, et al. Selective sexual dimorphism in musculoskeletal and cardiopulmonary pathologic manifestations and mortality incidence in the tumor necrosis factor-transgenic mouse model of rheumatoid arthritis. Arthritis Rheumatol 2019;71:1512–1523.
29. Mise-Omata S, Kuroda E, Niikura J, et al. A proximal kappaB site in the IL-23 p19 promoter is responsible for RelA- and c-Rel-dependent transcription. J Immunol 2007;179:6596–6603.
30. Kakoki M, Tsai YS, Kim HS, et al. Altering the expression in mice of genes by modifying their 3′ regions. Dev Cell 2004;6:597–606.
31. Lee HJ, Sinha AA. Cutaneous lupus erythematosus: understanding of clinical features, genetic basis, and pathobiology of disease guides therapeutic strategies. Autoimmunity 2006;39:433–444.
32. Gunawan M, Her Z, Liu M, et al. A novel human systemic lupus erythematosus model in humanised mice. Sci Rep 2017;7:16642.
33. Qiu W, Yu T, Deng GM. The role of organ-deposited IgG in the pathogenesis of multi-organ and tissue damage in systemic lupus erythematosus. Front Immunol 2022;13:924766.
34. Dean GS, Tyrrell-Price J, Crawley E, et al. Cytokines and systemic lupus erythematosus. Ann Rheum Dis 2000;59:243–251.
35. Lourenço EV, La Cava A. Cytokines in systemic lupus erythematosus. Curr Mol Med 2009;9:242–254.
36. King JK, Philips RL, Eriksson AU, et al. Langerhans cells maintain local tissue tolerance in a model of systemic autoimmune disease. J Immunol 2015;195:464–476.
37. Bitar C, Menge TD, Chan MP. Cutaneous manifestations of lupus erythematosus: a practical clinicopathological review for pathologists. Histopathology 2022;80:233–250.
38. Taylor GA, Carballo E, Lee DM, et al. A pathogenetic role for TNF alpha in the syndrome of cachexia, arthritis, and autoimmunity resulting from tristetraprolin (TTP) deficiency. Immunity 1996;4:445–454.
39. Ghosh S, Hoenerhoff MJ, Clayton N, et al. Left-sided cardiac valvulitis in tristetraprolin-deficient mice: the role of tumor necrosis factor alpha. Am J Pathol 2010;176:1484–1493.
40. Molle C, Zhang T, de Lendonck LY, et al. Tristetraprolin regulation of interleukin 23 mRNA stability prevents a spontaneous inflammatory disease. J Exp Med 2013;210:1675–1684.
41. Keffer J, Probert L, Cazlaris H, et al. Transgenic mice expressing human tumour necrosis factor: a predictive genetic model of arthritis. EMBO J 1991;10:4025–4031.
42. Hawkes JE, Yan BY, Chan TC, et al. Discovery of the IL-23/IL-17 signaling pathway and the treatment of psoriasis. J Immunol 2018;201:1605–1613.
43. Liu T, Li S, Ying S, et al. The IL-23/IL-17 pathway in inflammatory skin diseases: from bench to bedside. Front Immunol 2020;11:594735.
44. Cai Y, Xue F, Quan C, et al. A critical role of the IL-1β-IL-1R signaling pathway in skin inflammation and psoriasis pathogenesis. J Invest Dermatol 2019;139:146–156.
45. Vukelic M, Laloo A, Kyttaris VC. Interleukin 23 is elevated in the serum of patients with SLE. Lupus 2020;29:1943–1947.
46. Wang X, Liu X, Zhang Y, et al. Interleukin (IL)-39 [IL-23p19/Epstein-Barr virus-induced 3 (Ebi3)] induces differentiation/expansion of neutrophils in lupus-prone mice. Clin Exp Immunol 2016;186:144–156.